



ELSEVIER

Available online at www.sciencedirect.com

SCIENCE @ DIRECT®

Nuclear Instruments and Methods in Physics Research A 509 (2003) 340–345

**NUCLEAR
INSTRUMENTS
& METHODS
IN PHYSICS
RESEARCH**
Section Awww.elsevier.com/locate/nima

Large-scale images taken with the Medipix1 chip

K.-F.G. Pfeiffer^{a,*}, J. Giersch^a, G. Anton^a, L. Bätz^b, M. Hoheisel^b^aPhysikalisches Institut, Abt. 4, Universität Erlangen-Nürnberg, Erwin-Rommel-Strasse 1, 91058 Erlangen, Germany^bSiemens AG Medical Solutions, Competence Center X-Ray and Reconstruction Methods, Henkestr. 127, 91052 Erlangen, Germany

Abstract

Two methods to acquire large-scale X-ray images with high spatial resolution using the Medipix1 detector chip are presented. The Medipix1 chip is a pixelated, photon counting X-ray detector which was developed within the framework of the Medipix Collaboration.¹ Since the lateral dimensions of the Medipix1 chip are only 10.88 mm × 10.88 mm, larger images are acquired by tiling, which also helps to minimise the influence of defective pixels on the image quality.

Measurements on the modulation transfer function (MTF) and the detective quantum efficiency (DQE) of the detector were performed and first results are given. The MTF of the Medipix1 chip is quite close to the theoretical limit. The DQE is lower than expected and has to be investigated further.

© 2003 Elsevier Science B.V. All rights reserved.

PACS: 42.79.Pw; 87.57.Ce; 87.59.Hp; 87.57.–s

Keywords: Medipix; X-ray imaging; Large field; Photon counting; MTF; DQE

1. Detector and experimental setup

1.1. The Medipix1 detector

The Medipix1 detector is a pixelated solid state hybrid X-ray detector. It consists of a sensor layer (in our case 300 μm silicon) with 64 × 64 square pixels of 170 μm size, which is bump bonded to an equally pixelated read-out chip. It works in photon counting mode and has an adjustable energy threshold. Detailed description of the chip and the readout electronics can be found elsewhere [1,2].

1.2. Experimental setup

The X-ray source used is a mammographic X-ray tube with Mo anode (Siemens Mammomat B). All images were taken at 35 kV tube voltage and with 30 μm Mo + 2 mm Al filtering. Due to this filtering, the X-ray spectrum starts at a photon energy of about 15 keV and has a mean energy of 23.1 keV. The detector is mounted on two computer controlled translation stages for *x*–*y* positioning. Data acquisition is controlled by the Medisoft² software via the MUR0S1³ interface board [3]. Since the positioning accuracy of the translation stages is about 1 μm, which is much

*Corresponding author.

E-mail address: frieder.pfeiffer@physik.uni-erlangen.de

(K.-F.G. Pfeiffer).

¹<http://www.cern.ch/MEDIPIX>.

²Written by the University of Napoli-INFN group, Italy.

³Developed by NIKHEF, Amsterdam, The Netherlands.

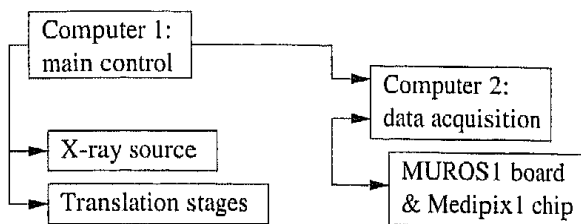


Fig. 1. Schematic view of the setup with control and data acquisition structures.

better than the pixel size of $170\ \mu\text{m}$, they can be used for seamless image tiling and there are no misalignment artifacts in the resulting large images. The complete system is automated⁴ so that multiple images can be taken quite easily (Fig. 1).

2. Large-field images

Because of the quite small size of the Medipix1 chip ($10.88\ \text{mm} \times 10.88\ \text{mm}$) compared to typical objects to be examined, one needs to find a way to generate large images from single detector-sized sub-images. In the following, two basic methods will be described and the particular advantages of each will be pointed out.

2.1. "Move and tile"

This method is a straightforward application of the x - y translation stages. To cover an object larger than the Medipix1 chip, the necessary field of view is scanned with the chip until the whole area has been imaged (Fig. 2). The scanning steps can be chosen as appropriate. If there is an overlap between two images, dead pixels in one image can be replaced by data taken from the other one. The advantage of this method can be clearly seen by comparing Fig. 3, which shows a single image with some defective pixels, with Fig. 4, which shows a larger tiled image of a radial resolution phantom (a so-called 'Siemensstar'⁵). Here none of these defective pixels can be seen because of the data

⁴The server-client programs used were written by Ch. Bert and D. Niederlöhner, Universität Erlangen-Nürnberg.

⁵0.05 mm lead embedded in 2 mm PMMA, 2° segmentation, \varnothing 45 mm.

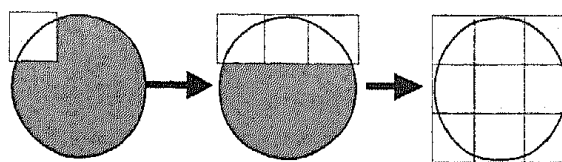


Fig. 2. Move and tile method: schematic process of image acquisition.

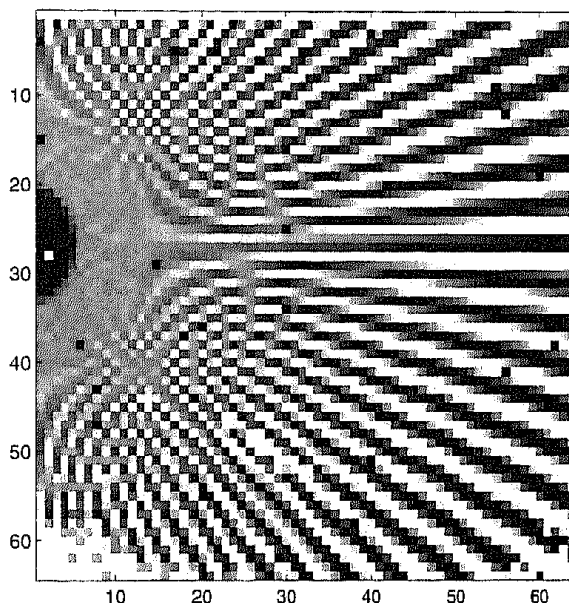


Fig. 3. Move and tile method: detector-sized single sub-image which shows some single dead pixels, the defective first row and the defective lower left corner (white pixels).

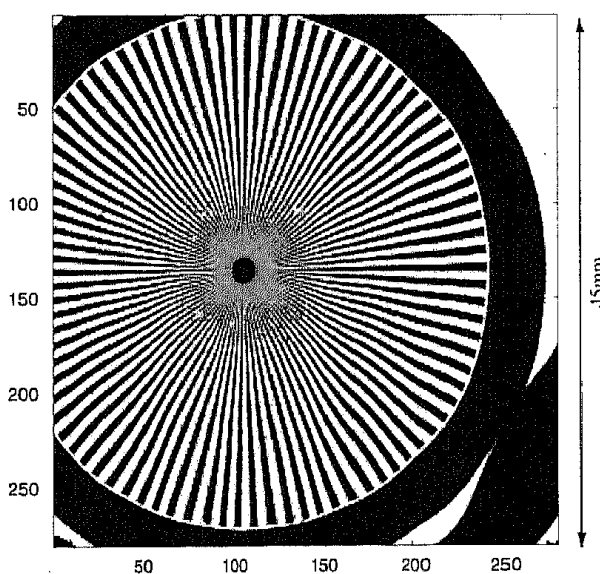


Fig. 4. Move and tile method: 5×5 images with 10 pixels overlap to get rid of the defective first row and the defective pixels in the lower left corner of the detector. The object imaged here is a so-called 'Siemensstar'.

replacement. Since the detector has a very large linear range and the image data consists of the number of counted photons, data handling is very easy and pixel-wise data averaging is simply done by calculating mean values (as is done, e.g. in Fig. 4). Because fluctuations in the X-ray dose emitted by the tube can occur, each sub-image should be normalized accordingly.

This method is referred to as “*move and tile*”, because the detector is first *moved* to different positions and the whole image is made up of the single *tiles* at the end. An example for this method can be seen in Fig. 4. Fig. 5 shows the profile along pixel row 190 of Fig. 4 and demonstrates the high contrast even for small details.

This method is very flexible for different object sizes and geometries, the main advantage being that only a single detector with readout electronics is needed. However, the larger the object is, the longer it takes and the more dose is applied. Therefore, it is suitable for lab applications and detector testing, but not really useful for industrial or medical applications.

2.2. “*Tile and move*”

In order to image larger objects more effectively a second method has been applied: at first several detectors are tiled in a fixed array, which results in a large field image with small gaps. To cover the gaps in the image, the detector array is then moved twice diagonally so that the overlay of three pictures shows no gaps anymore. Thus, only three exposures are needed (provided that the gaps are less than half the detector chip size) and

the resulting image has a quite high photon statistics in the overlapping areas leading to a better signal-to-noise ratio (SNR). The drawbacks of this method are the larger number of single detectors needed and—to a lesser extent—the high data rate because the whole detector array should be read out as fast as possible. Nevertheless, it also has the advantage that only a single translation stage is required for moving the detector array. This method is referred to as “*tile and move*”, because first several detectors are *tiled* into a fixed array, which is subsequently *moved* to gather all data.

In Fig. 6 the method is schematically shown, whereas Fig. 7 is an actual measurement which clearly shows the gaps in the detector array. Because only one chip was available, the tiled array has been simulated using the translation stages to scan the fixed chip positions within the array. Fig. 8 is the merged image of the ‘Siemensstar’.

3. Detector performance

In order to compare different sensors or imaging methods, it is essential to agree on a set of parameters to describe the image quality. The modulation transfer function (MTF) describes the spatial frequency response of the imaging system, whereas the frequency-dependent detective quantum efficiency (DQE) can be defined as $DQE(f) = SNR_{out}^2(f)/SNR_{in}^2(f)$. The concepts of MTF and DQE have been explained in detail by Cunningham [4] and are now widely used for describing detector performance.

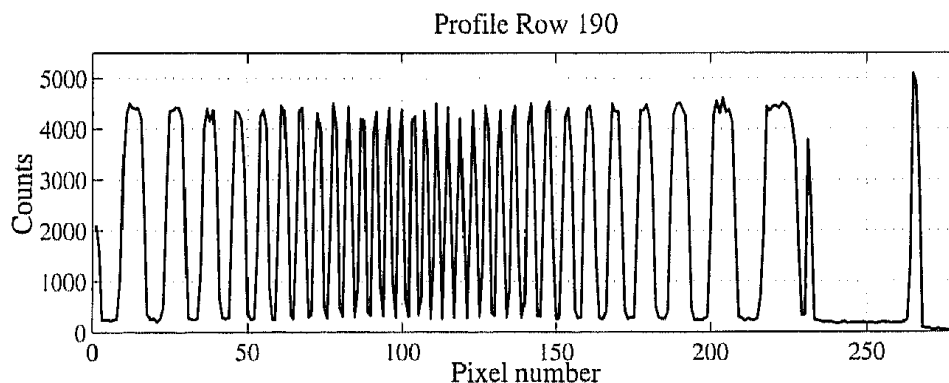


Fig. 5. Move and tile method: profile of row 190; peak-to-peak distance at the centre ~ 0.6 mm.

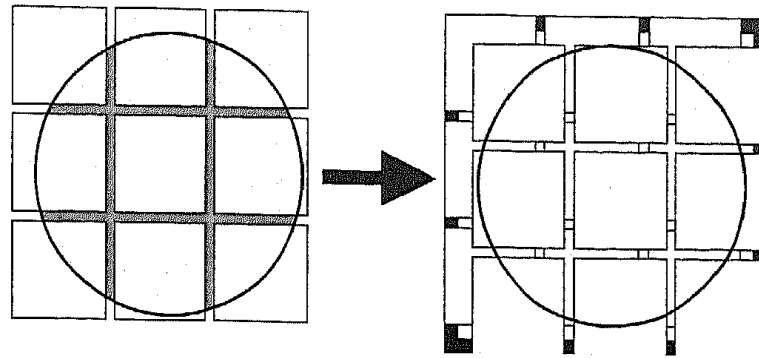


Fig. 6. Tile and move method: schematic process of image acquisition. The black areas on the edges are not covered by the final image.

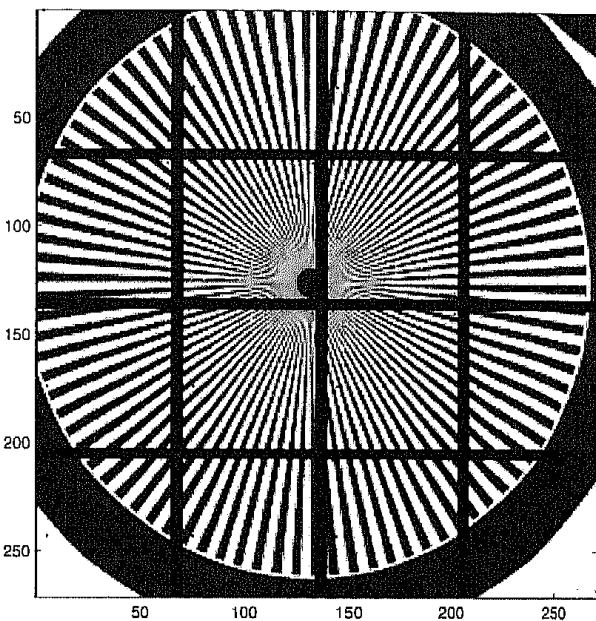


Fig. 7. Tile and move method: single frame consisting of 4×4 detectors.

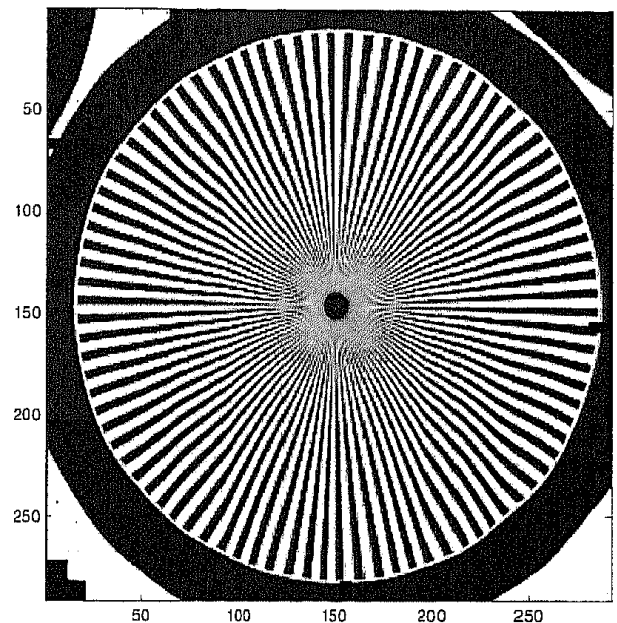


Fig. 8. Tile and move method: merged image from three frames. The lower left corner is part of the areas not covered by any of the frames.

3.1. MTF

For measuring the MTF of the Medipix1 detector, a large image (width 15.5 cm) of a lead bar pattern⁶ was taken using the move and tile method (Fig. 9). From this image, the modulation values of a rectangular excitation have been extracted and the MTF has been subsequently calculated as described elsewhere [5,6].

The theoretical limit for square pixels is given by $\text{sinc}(\pi fl) = \sin(\pi fl)/(\pi fl)$, where f denotes the spatial frequency and l the (effective) pixel side

length. Comparing the results of the measurement with theoretical values for square pixels with different sizes, one can estimate the effective pixel size to be a little less than $170 \mu\text{m}$. This can be attributed to the effect of charge sharing (see Section 3.2). Fig. 10 shows the measured data in comparison to theoretical values for 170 and $165 \mu\text{m}$ pixel size, respectively.

3.2. Detective quantum efficiency

The method to determine the DQE has been described in detail by Dobbins III [6]. In order to determine the DQE, the noise power spectrum

⁶Type 40 fabricated by Hüttner, Heroldsbach, Germany, spatial frequency range $0.05 - 10 \text{ lp/mm}$.

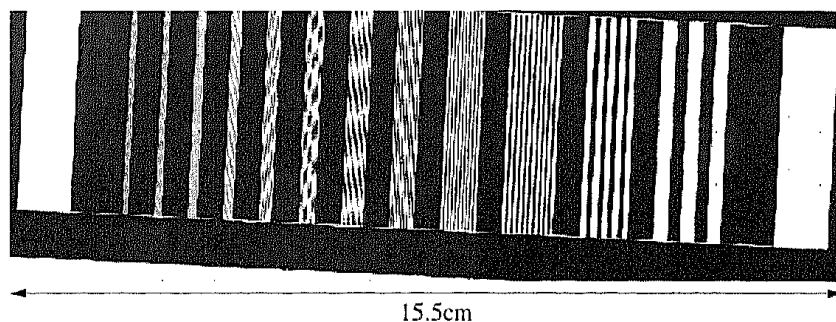


Fig. 9. Measurement of the line pair phantom for the evaluation of the MTF.

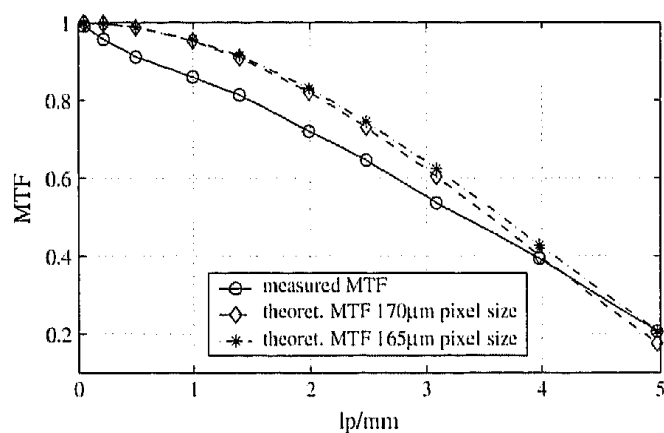


Fig. 10. MTF of the detector in comparison to theoretical values for 170 and 165 μm pixel size.

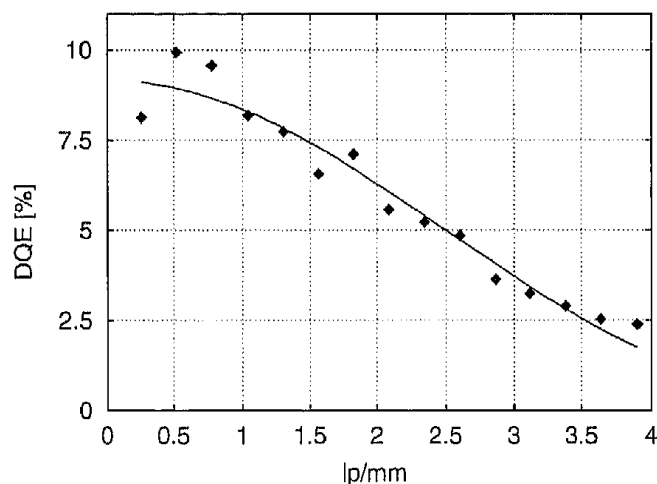


Fig. 11. The DQE of a Medipix1 chip with a 300 μm Si detector layer and a tube voltage of 35 kV (30 μm Mo + 2 mm Al filtering).

(NPS) is also needed. Several homogeneously irradiated images were taken to form a large flat field image, from which the NPS was calculated as

the modulus square of the two-dimensional Fourier transform of quadratic (32×32 pixels) overlapping subregions.

For comparing the measured DQE values (see Fig. 11) to those of other detectors the rather low absorption probability of 300 μm Si for the given photon spectrum has to be taken into account (23.8% of the incident quanta are expected to be absorbed). The spectrum of the X-ray source has been calculated according to Boone [7]. However, in the flat field images only 81.5% of the expected quanta were detected, which can be explained by an effective pixel side length of less than 170 μm (cf. the MTF evaluation). The loss in active area may be partly due to incomplete charge collection—but this should be only a minor correction—and is mainly due to the process of charge sharing. If a photon hits the sensor near the boundary between pixels, the generated charge is divided between the neighbouring pixels, effectively suppressing the photon: none of the partial signals is large enough to pass the respective pixel discriminator and trigger the counter. Hence, this effect is also influenced by the setting of the discriminator level. For more detailed studies on charge sharing see for example Refs. [8,9].

Fig. 11 shows the DQE of the Medipix1 chip we have examined with a 300 μm Si detector layer and a tube voltage of 35 kV (30 μm Mo + 2 mm Al filtering⁷). The data is still quite noisy because of the low statistics which were available for the calculation.

⁷Thus, the lowest photon energy is about 15 keV, which is well above the detection threshold of the chip. The mean energy of the spectrum is 23.1 keV.

4. Summary and outlook

Two methods to image large objects using the Medipix1 chip have been presented and discussed. In addition, first results for the MTF and DQE of the detector assembly have been obtained. Further investigation of image quality is planned as well as similar measurements using the Medipix2 chip [10], which will be available soon.

References

- [1] M. Campbell, E.H.M. Heijne, G. Meddeler, E. Pernigotti, W. Snoeys, *IEEE Trans. Nucl. Sci.* 45 (3) (1998) 751.
- [2] B. Mikulec, M. Campbell, G. Dipasquale, C. Schwarz, J. Watt, *Nucl. Instr. and Meth. A* 458 (2001) 352.
- [3] G. Bardelloni, E. Bertolucci, A.L.J. Boerkamp, D. Calvet, M. Conti, M. Maiorino, P. Russo, J.L. Visschers, *IEEE Nucl. Sci. Symp. Med. Imaging Conf.* 12 (2000) 57.
- [4] J. Beutel, H.L. Kundel, R.L.V. Metter (Eds.), *Handbook of Medical Imaging, Vol. 1 Physics and Psychophysics*, SPIE Press, 2000, pp. 79–159 (Chapter 2, Applied Linear-Systems Theory).
- [5] J.W. Coltman, *J. Opt. Soc. Am.* 44 (6) (1954) 468.
- [6] J. Beutel, H.L. Kundel, R.L.V. Metter (Eds.), *Handbook of Medical Imaging, Vol. 1, Physics and Psychophysics*, SPIE Press, Bellingham, Washington, 2000, pp. 161–222 (Chapter 3, Image Quality Metrics for Digital Systems).
- [7] J. Boone, T. Fewell, R. Jennings, *Med. Phys.* 24 (12) (1997) 1863.
- [8] C. Ponchut, J.L. Visschers, A. Fornaini, H. Graafsma, M. Maiorino, G. Mettivier, D. Calvet, *Nucl. Instr. and Meth. A* 484 (2002) 396.
- [9] M. Chmeissani, B. Mikulec, *Nucl. Instr. and Meth. A* 460 (2001) 81.
- [10] M. Campbell, First test measurements of a 64k pixel readout chip working in single photon counting mode, Talk presented at IWoRID 2002, Amsterdam, September 2002.